U.S. Department
of Transportation

**Urban Mass
Transportation
Administration**

UMTA-MA-06-0025-83-11
DOT-TSC-UMTA-83-7

Algorithms and Parametric Studies for Assessing Effects of Two-Point Contact

John A. Elkins

The Analytic Sciences Corporation
One Jacob Way
Reading MA 01867

February 1984
Final Report

UMTA Technical Assistance Program

Technical Report Documentation Page

1. Report No.	2. Government Accession No.	3. Recipient's Catalog No.
UMTA-MA-06-0025-83-11	PB84-182799	

4. Title and Subtitle

Algorithms and Parametric Studies for Assessing Effects of Two-Point Contact

5. Report Date	6. Performing Organization Code	8. Performing Organization Report No.
February 1984	TSC/DTS-76	DOT-TSC-UMTA-83-7

7. Author(s)

John A. Elkins

9. Performing Organization Name and Address

The Analytic Sciences Corporation*
One Jacob Way
Reading, Massachusetts 01867

10. Work Unit No. (TRAIS)	11. Contract or Grant No.	13. Type of Report and Period Covered
MA-06-0025(UM377/R3691)	DTRS-57-80-C-00062	Final Report March 1982 - August 1982

12. Sponsoring Agency Name and Address

U.S. Department of Transportation
Urban Mass Transportation Administration
400 Seventh Street, S.W.
Washington, D. C. 20590

14. Sponsoring Agency Code

URT-10

15. Supplementary Notes

*Under contract to: U.S. Department of Transportation
Research and Special Programs Administration
Transportation Systems Center
Cambridge, Massachusetts 02142

16. Abstract

This report describes analyses conducted to assess the effects of two-point wheel rail contact on a single wheel on the prediction of wheel-rail forces, and for including these effects in a computer program for predicting curving behavior of rail vehicles. This condition exists for conventional wheel profiles when the wheel is in flange contact with one point of contact being on the tread and the second on the flange. The condition also exists and is particularly significant when conventional wheels come into flange contact or a restraining rail is used to prevent flange contact. The analytical approaches in current use are reviewed and the predictions of computer programs using these approaches are compared to data obtained in recent tests conducted on track of the Washington Metropolitan Area Transit Authority in Washington, D.C. The analyses are incorporated into computational algorithms and a computer program for predicting wheel rail forces in curve negotiation. The program is applied to development of curving force predictions for a typical transit car operating over track with and without restraining rail.

This work has indicated that significant reductions in wheel-rail wear and train resistance in curves would probably be available from wheel profiles which give only a single point of contact with the rail.

17. Key Words	18. Distribution Statement
Algorithms; Computer Programs; Curve Negotiation; Curves and Curving; Parametric Studies; Rail Transit; Rail-Wheel Profiles; Restraining Rail; Two-Point Wheel-Rail Contact; Washington Metropolitan Area Transit Authority; Wheel-Rail Forces	**Available to the Public through the National Technical Information Service, Springfield, Virginia 22161.**

19. Security Classif. (of this report)	20. Security Classif. (of this page)	21. No. of Pages	22. Price
Unclassified	**Unclassified**	27	A03

Technical Report Documentation Page

1. Report No.	2. Government Accession No.	3. Recipient's Catalog No.
UMTA-MA-06-0025-83-11		

4. Title and Subtitle
ALGORITHMS AND PARAMETRIC STUDIES FOR ASSESSING EFFECTS OF TWO-POINT CONTACT

5. Report Date
February 1984

6. Performing Organization Code
TSC/DTS-76

7. Author(s)
John A. Elkins

8. Performing Organization Report No.
DOT-TSC-UMTA-83-7

9. Performing Organization Name and Address
The Analytic Sciences Corporation*
One Jacob Way
Reading, MA 01867

10. Work Unit No. (TRAIS)
UM377/R3691

11. Contract or Grant No.
DTRS-57-80-C-00062

12. Sponsoring Agency Name and Address
U.S. Department of Transportation
Urban Mass Transportation Administration
Office of Technical Assistance
Washington, DC 20590

13. Type of Report and Period Covered
Final Report
March 1982-August 1982

14. Sponsoring Agency Code
URT-10

15. Supplementary Notes
*Under contract to: U.S. Department of Transportation
Research and Special Programs Administration
Transportation Systems Center
Cambridge, MA 02142

16. Abstract

Analyses are presented for predicting the effects of two-point contact of a single wheel on wheel rail forces developed in negotiation of curves by rail vehicles. This condition exists for conventional wheel profiles when the wheel is in flange contact with one point of contact being on the tread and the second on the flange. The condition also exists when a restraining rail is employed when the second point of contact is on the back of the flange. The analyses are incorporated into computational algorithms and a computer program for predicting wheel rail forces in curve negotiation. The program is applied to development of curving force predictions for a typical transit car operating over track with and without restraining rail. The results without restraining rail are shown to be in good agreement with recently obtained test data.

17. Key Words	18. Distribution Statement
Curve Negotiation, Rail Wheel Profiles, Restraining Rail, Rail Transit	DOCUMENT IS AVAILABLE TO THE PUBLIC THROUGH THE NATIONAL TECHNICAL INFORMATION SERVICE, SPRINGFIELD, VIRGINIA 22161

19. Security Classif. (of this report)	20. Security Classif. (of this page)	21. No. of Pages	22. Price
UNCLASSIFIED	UNCLASSIFIED	28	

PREFACE

In support of the Office of Technical Assistance of the Urban Mass Transportation Administration (UMTA), the Transportation Systems Center (TSC) is conducting analytical and experimental studies to relate transit truck design characteristics and wheel rail forces and wear in order to provide options for decreasing wear rates of wheels and rails experienced by transit properties. Such reduced wear rates aid in minimzing vehicle and track system life-cycle costs while maintaining or improving equipment performance.

Under contract to Transportation Systems Center, The Analytic Sciences Corporation (TASC) has been providing support in analysis and test design of these efforts. Tests were recently conducted by TSC to determine the influence of truck primary suspension stiffness variations and wheel profile variations on the wheel rail lateral forces produced by rail transit vehicles on track of the Washington Metropolitan Area Transit Authority. The test results indicated that there was a significant difference between the measured influence of wheel profile on wheel rail forces and that predicted by current analytic methods. A review of the analytic approaches indicated that the effects of two-point contact (tread and flange) were either omitted or oversimplified in current analytic methods. Accordingly, TASC conducted a review of the modeling techniques in current use and conducted analyses to extend the existing methods to include the effects of two point contact.

This report describes the work conducted to develop algorithms for handling the two point contact situation and the revision of computer programs to predict curving behavior to include these situations.

The author would like to thank Dr. Herbert Weinstock, the TSC technical monitor and Dr. F.B. Blader of TASC for their helpful discussion of the problem.

SUMMARY

This report describes analyses conducted to assess the effects of two-point wheel rail contact on a single wheel on the prediction of wheel-rail forces, and for including these effects in a computer program for predicting curving behavior of rail vehicles. The two point contact effects are particularly significant when conventional wheels come into flange contact or a restraining rail is used to prevent flange contact.

The analytic approaches in current use are reviewed and the predictions of computer programs using these approaches are compared to data obtained in recent tests conducted on track of the Washington Metropolitan Area Transit Authority. This review, supported by the test data, indicated that the models of curving performance which did not take two-point contact effects into account, or had only a rudimentary representation of the profiles, failed to predict accurately the effects of wheel-rail profile variations on changes in curving behavior.

When the axle of rail car comes into flange contact a significant steering moment arises which tends to turn the axle towards the center of the track. The use of a single point of contact analysis where two points of contact exist tends to produce an estimate of this steering moment that is larger than will actually occur and therefore wheel-rail force estimates that are too low. This report discusses the influence of wheel-rail profile and two-point contact on the wheelset force and steering moment characteristics.

The results of the analyses of wheelset force and moment behavior are incorporated into computational programs for predicting curving behavior for both wheel flanging and restraining rail conditions. The forces predicted by these computer programs are compared to data obtained in the WMATA tests and are shown to be in very good agreement with the experimental data.

The computer program is also applied to prediction of wheel-rail forces with restraining rail as a function of curve radius and speed for an unlubricated restraining rail. The results indicate that the restraining rail, if unlubricated, will support a significant portion of vertical load, tending to reduce the load on the low rail. Lateral forces on the restraining rail are predicted to be comparable to those that would exist on the high rail if the restraining rail were not present. The results of the restraining rail analyses will be compared at a later date with test data on a 150-ft curve, with and without restraining rail, that is currently being obtained by Transportation Test Center in Pueblo, Colorado using the UMTA "State of the Art Car" (SOAC).

METRIC CONVERSION FACTORS

Approximate Conversions to Metric Measures

Symbol	When You Know	Multiply by	To Find	Symbol
	LENGTH			
in	inches	*2.5	centimeters	cm
ft	feet	30	centimeters	cm
yd	yards	0.9	meters	m
mi	miles	1.6	kilometers	km
	AREA			
in^2	square inches	6.5	square centimeters	cm^2
ft^2	square feet	0.09	square meters	m^2
yd^2	square yards	0.8	square meters	m^2
mi^2	squers miles	2.6	square kilometers	km^2
	acres	0.4	hectares	he
	MASS (weight)			
oz	ounces	28	grams	g
lb	pounds	0.45	kilograms	kg
	short tons (2000 lb)	0.9	tonnes	t
	VOLUME			
tsp	teaspoons	5	milliliters	ml
Tbsp	tablespoons	15	milliliters	ml
fl oz	fluid ounces	30	milliliters	ml
c	cups	0.24	liters	l
pt	pints	0.47	liters	l
qt	quarts	0.95	liters	l
gal	gallons	3.8	liters	l
ft^3	cubic feet	0.03	cubic meters	m^3
yd^3	cubic yards	0.76	cubic meters	m^3
	TEMPERATURE (exact)			
°F	Fahrenheit temperature	5/9 (after subtracting 32)	Celsius temperature	°C

*1 in = 2.54 (exactly). For other exact conversions and more detailed tables, see NBS Misc. Publ. 286, Units of Weights and Measures, Price $2.25, SD Catalog No. C13.10:286.

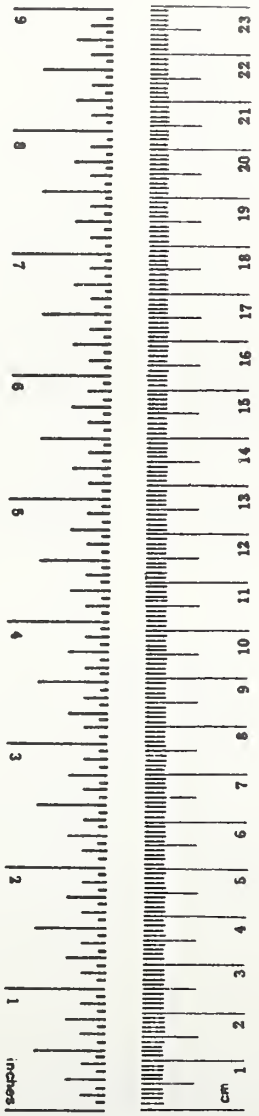

Approximate Conversions from Metric Measures

Symbol	When You Know	Multiply by	To Find	Symbol
	LENGTH			
mm	millimeters	0.04	inches	in
cm	centimeters	0.4	inches	in
m	meters	3.3	feet	ft
m	meters	1.1	yards	yd
km	kilometers	0.6	miles	mi
	AREA			
cm^2	square centimeters	0.16	square inches	in^2
m^2	square meters	1.2	square yards	yd^2
km^2	square kilometers	0.4	square miles	mi^2
ha	hectares (10,000 m^2)	2.5	acres	
	MASS (weight)			
g	grams	0.035	ounces	oz
kg	kilograms	2.2	pounds	lb
t	tonnes (1000 kg)	1.1	short tons	
	VOLUME			
ml	milliliters	0.03	fluid ounces	fl oz
l	liters	2.1	pints	pt
l	liters	1.06	quarts	qt
l	liters	0.26	gallons	gal
m^3	cubic meters	35	cubic feet	ft^3
m^3	cubic meters	1.3	cubic yards	yd^3
	TEMPERATURE (exact)			
°C	Celsius temperature	9/5 (then add 32)	Fahrenheit temperature	°F

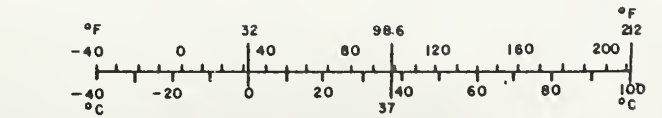

TABLE OF CONTENTS

LIST OF FIGURES

1. INTRODUCTION

The problem of calculating the forces that guide a railroad axle has been the subject of much study over the last century. There has been particular interest in the prediction of forces occurring during the negotiation of curves, because of the large forces that can be generated in this circumstance. In particular, the high rates of wheel and rail wear, which lead to large expenditures on maintenance and renewal, are of special concern.

The ability to predict the forces at the wheel/rail interface and the consequent rates of wheel and rail wear is important to the understanding and possible alleviation of these problems. Separate approaches for modeling the wheel/rail interaction have been used by different investigators for predicting the wheel/rail forces which occur in curve negotiation, and for estimating wheel/rail wear. Until recently, insufficient data existed for complete experimental verification of the predictions of the various models. Tests conducted by British Rail, which were reported by Elkins and Gostling in 1977 (Ref. 1), showed excellent agreement with predictions using a single point contact representation of the actual wheel and rail profiles. However, an attempt to apply the same analysis directly to evaluating the influences of wheel profile changes on the curving performance of transit trucks (Ref. 2), failed to yield agreement with experimental observations.

Accordingly, a review of the modeling approaches in current use was conducted, to attempt to find the reasons for this discrepancy. It showed that the single point of contact assumption was a gross mathematical approximation for the new wheel and rail profiles in current use on U.S. railroads and transit properties. For these wheel profiles, the curving behavior is dominated by wheel/rail contact at two points on the leading axle wheel at the high rail.

It is common practice on some transit properties to use a restraining rail on the sharper curves. The purpose of the restraining rail being to reduce gauge face wear on the high rail and to prevent derailment. The use of a restraining rail also results in a two-point contact situation on a single wheel. In this case, the second point of contact is on the back face of the flange rather than the front face.

This report reviews the assumptions of the modeling approaches, which are used currently for the prediction of the curving behavior of rail vehicles and presents the results of an improved modeling approach, which takes the effects of two-point contact more fully into account. These results are compared with data recently obtained from curving tests (Ref. 2) that were conducted by the Transportation Systems Center (TSC) for the Urban Mass Transportation Administration (UMTA) on track and equipment of the Washington Metropolitan Area Transit Authority (WMATA).

2. HISTORICAL BACKGROUND

Prior to the 1960's, steady-state curving predictions were performed using a method published, posthumously, by Porter in 1935 (Ref. 3). This method evolved from work commenced by Mackenzie in 1883 (Ref. 4) and pursued by many different workers in the intervening years. The treads of each wheel were considered to be cylindrical and forces were developed by sliding friction. The direction of the force was aligned with the direction of the slippage vector. Additional lateral forces were developed by the flange when it came into contact with the gauge face of the rail.

During the 1960's, there was a strong interest in the development of high speed ground transportation in Europe, Japan, and the United States. As a result, intensive research commenced into the nature of the forces taking place at the wheel/rail interface. Initially, this work was directed towards a fuller understanding of the hunting phenomenon. Modeling of the wheel/rail forces as linear functions of creepage by Wickens (Ref. 5) led to the ability to predict the onset of hunting, and demonstrated that it was a dynamic instability, akin to the flutter of aircraft lifting surfaces.

Later, the linear relationships between creep force and creepage were also applied to the problem of predicting the curving behavior of railroad vehicles by Boocock (Ref. 6) and Newland (Ref. 7). To establish the limits of applicability, boundaries were established, beyond which either flange contact or slippage would occur. In both the curving analyses and the hunting studies, the wheel/rail geometry was represented by linear functions and contact with the flange was considered to be a limiting case.

The curving models were later refined to include the effects of gravitational stiffness and spin creep, which were shown to be significant with worn or profiled wheels, particularly when contact occurred close to the flange root. The analyses conducted using the linear creep theory considered flange contact as a condition to be avoided and, therefore, at the limit of the analysis. However, the limitation occurred for almost all vehicles on curves having a radius of smaller than 2,000 ft (3°), and for most vehicles on much larger radius curves, whereas the major problems of rail wear and track damage were occurring on smaller radius curves.

At this point two different approaches were pursued. The desire to have wheel profiles which would remain approximately the same shape throughout their life, led to the development of profiled wheels. These profiles were found to give only a single point of contact with the rail for most of the rail profiles, new or worn, found in practice. In order to evaluate the performance of these profiled wheels, detailed analytical models of the wheel/rail interaction were developed. These models made use of Kalker's nonlinear creep theory (Ref. 8), which had become available at about this time. As a result, the nonlinearities arising from both the single point contact wheel/rail geometry and the creep force creepage relationships, inherent in Kalker's nonlinear theory, were modeled. This approach is described in the work of Gilchrist and Brickle (Ref. 9), Elkins and Gostling (Ref. 1) and Sweet and Sivak (Ref. 10). Experimental results for lateral force and yaw moment were obtained from both full scale experiments and model tests, which gave good agreement with the predicted wheel/rail forces.

In the United States, a different approach was pursued. The concepts of Porter and Boocock-Newland were combined, to produce a model which calculated tread forces from the linear creep force relationships for a straight tapered wheel, and introduced a lateral force on an implicitly vertical flange (Refs. 11, 12).

The predictions from this method were compared with measured wheel/rail lateral forces (Refs. 11, 12) and by selecting suitable values for the wheel/rail friction coefficient and making certain assumptions with regard to the centerplate friction torque, it was possible to obtain reasonable agreement with the measurements of high rail lateral force. However, the sign of the centerplate friction torque that was assumed was of the opposite sign to that likely to be occurring in practice. In addition, the single-point contact models, described previously, predicted a large increase in steering moment, once contact on the flange occurred and this was substantiated by the experimental results from both full scale and model tests (Refs. 1, 10, 13).

The vertical flange assumption neglected the steering moment, that occurs once flange contact takes place and gave a moment coming entirely from the tread, which was in the opposite direction to that frequently occurring following flange contact. In order to overcome this deficiency, the concept of a flange friction coefficient was introduced, which gave a longitudinal force on the flange proportional to the lateral flange force. This longitudinal flange force gives a steering moment on the axle. (Ref. 14).

3. CURVING TESTS ON TRANSIT VEHICLES

Recently, several mass transit railroad systems have encountered problems of high rates of wheel and rail wear. One particular transit system that has encountered these problems is the Washington Metropolitan Area Transit Authority (WMATA). In view of the cost of maintenance resulting from the high rates of wear and the implications for other transit authorities, the Urban Mass Transportation Administration (UMTA) sponsored a test program to investigate the problem.

During Phase I, measurements of wheel/rail forces were made at two sites on the WMATA system, in order to determine the cause of the problem and to identify possible means of alleviation (Refs. 15 and 16). The WMATA vehicles were running with an AAR cylindrical wheel on AREA 115RE rail as standard, and during the test program the effect of changing to a British Rail 1 in 20 profile, with a filled-in flange root, was tested. In addition, a change in track gauge on curves was investigated.

Theoretical predictions of curving behavior were carried out by Weinstock and Greif (Ref. 17) using the vertical flange-model with flange friction. They were able to obtain reasonable agreement with the level of wheel/rail lateral forces being measured with the cylindrical wheel. However, they were unable to predict the relatively large reductions in lateral force that were measured with the British Rail 1 in 20

wheel profile. At the time, this discrepancy was attributed to the increased effective conicity of the British Rail 1 in 20 wheel profile, when contact was near to the flange root, and to the primary yaw stiffness of the truck being lower in practice than had been assumed in the predictions.

In addition to the situation at WMATA, the Metropolitan Atlanta Rapid Transit Authority (MARTA) had experienced similar problems during the early service life of their vehicles. As a result, a test program had been carried out at the Transportation Test Center (TTC) in Pueblo, Colorado (Ref. 18). During this test program, wheel/rail forces and angles-of-attack were measured. The effects of a modification to reduce the longitudinal stiffness of the primary suspension bush and a change in wheel profile were tested. In addition, the effect of axle misalignment was investigated, because it had been noted that some trucks were experiencing particularly high rates of wheel wear and that this was occurring asymmetrically.

The test results were compared with the theoretical predictions from a single point contact model of the truck curving behavior. Good agreement between theory and experiment was obtained on the basis of test results from a 7.4° curve. In this case, the changes in wheel profile appeared to have little effect on the curving performance.

A further Phase II test program was planned at WMATA, which included an effort to define and evaluate better modifications to the truck primary suspension along with changes in wheel profile. Tests were carried out over a route which included a number of curves in the range from 2° to 7.6° of curvature. The test truck was instrumented to measure primary suspension displacements, and a single instrumented wheelset was used to give a continuous measure of vertical and lateral force on both of the two wheels of the axle. Test runs were carried out in both the forward and reverse direction so that the instrumented wheelset was alternatively in the leading and trailing position.

The measured values from the instrumented wheelset were reduced to mean values in each of the curved test zones. These results were plotted against track curvature for each test configuration. With the standard primary suspension bush, tests were carried out with the AAR cylindrical and the British Rail 1 in 20 profile. Figure 3-1 shows the mean value of high

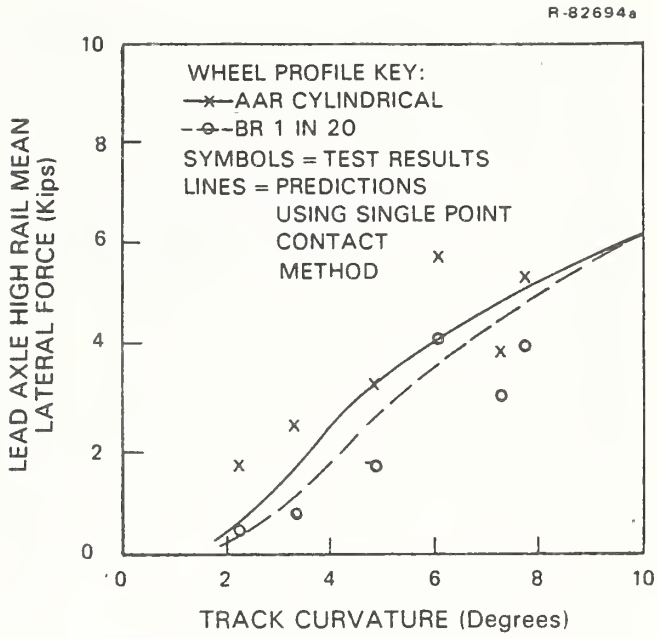

Figure 3-1 Lead Axle High Rail Lateral Force - Track Curvature (Stiff Suspension)

rail lateral force plotted against track curvature for the two different wheel profiles.

The test results indicate the magnitude of improvement in steady curving behavior obtained as a result of wheel profile change with the standard primary suspension bush. It is seen that the British Rail 1 in 20 profile offers a reduction in mean lateral force of approximately 27% for the sharpest curve compared with the AAR cylindrical wheel.

Predictions using the single point contact method indicate agreement with the measured force for the cylindrical wheel, approximately 4.9 Kips on a 7.6 degree curve with a wheel/rail friction coefficient of 0.5. However, the predictions show only a minor improvement with change in wheel profile. A reduction of only 4% was predicted for the sharpest curve compared with the 27% measured.

The primary suspension bush was modified to give a substantially lower yaw stiffness to improve curving performance. The modified bush gave a yaw stiffness of 30×10^6 lb-in/rad compared with 118×10^6 lb-in/rad for the standard bush.

Figure 3-2 illustrates high rail lateral force as a function of track curvature with the modified primary bush. Again, these are values for the

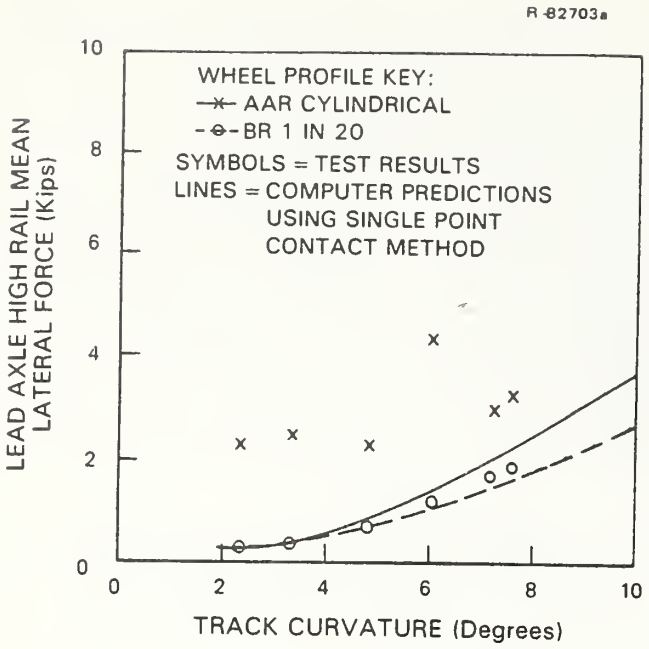

Figure 3-2 Lead Axle High Rail Lateral Force - Track Curvature (Soft Suspension)

balance speed on each curve. Mean curving forces, with respect to the standard suspension have been reduced by 36% and 65% in the sharpest curve by the cylindrical wheel and British Rail 1 in 20, respectively. It is seen that moderate reductions in force have been obtained by modifying the primary suspension with the AAR cylindrical wheel. However, dramatic reductions are obtained with the British Rail 1 in 20 wheel.

Theoretical predictions using the single-point contact method, indicated approximately the right magnitude of force compared with the experimental results for the British Rail 1 in 20 profile, but again predict relatively small changes with wheel profile. As a result, the predictions for the AAR cylindrical wheel are substantially less than those measured; 2 Kips mean lateral force was predicted compared with 3.3 Kips measured for the sharpest curve.

The large mean curving forces, occurring on the sharpest curve, cause high rates of wear, particularly on the gauge face of the high rail. Figure 3-3 shows a cross-sectional measurement at a site on the high rail of the sharpest (7.6°) curve compared with a new rail. It should be noted that the predictions of curving behavior were performed using the new rail profile, which as Fig. 3-3 shows, is significantly different from the measured profile. However, for both the new rail profile and the measured worn rail profile, two points of contact exist between the leading outer wheel on a curve and the high rail, with the AAR cylindrical profile. For the British Rail 1 in 20 profile, two-point contact occurs on the new rail, but on the worn rail the contact is single point, apart from a very small region of two-point contact.

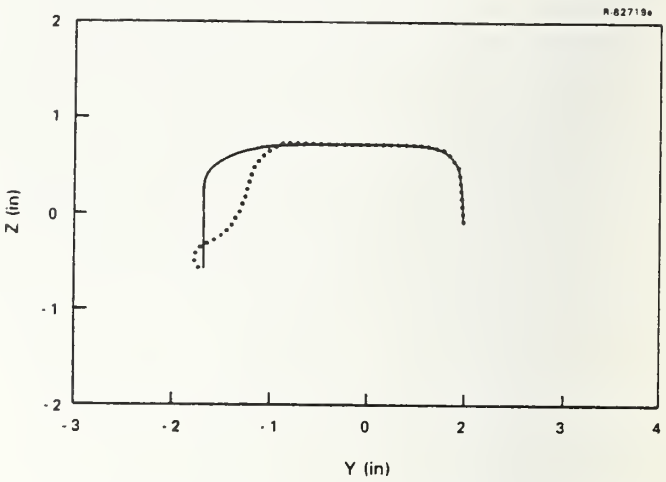

Figure 3-3 Measure High Rail Profile on a Curve 37 (7.6° Curvature) Compared with New Rail

4. WHEEL/RAIL MODEL

4.1 GENERAL

As a result of the discrepancies between calculated and observed results, a reexamination of the various methods of predicting wheel/rail forces was undertaken. In particular, it was noted that relatively large changes in wheel/rail lateral force were being measured with different wheel profiles, whereas predictions using a single point contact model were indicating only minor changes

The wheel/rail profile combinations that are in common use in the U.S.A. and in many other parts of the world almost invariably have two points of contact between the flanging wheel and high rail during curve negotiation.

The creepages and resulting creep force that occur at the interface between a wheel and rail when there is only a single point of contact are described in detail by Elkins Eickhoff (Ref. 19). The analysis that follows considers the situation where there are two points of contact between a single wheel and rail.

In the first case, the second point of contact is on the front face of the

flange. Typically, this occurs on the lead axle of a truck in a curve where the wheel in contact with the high rail is almost invariably in flange contact (Figs. 4.1-1 and 4.1-2).

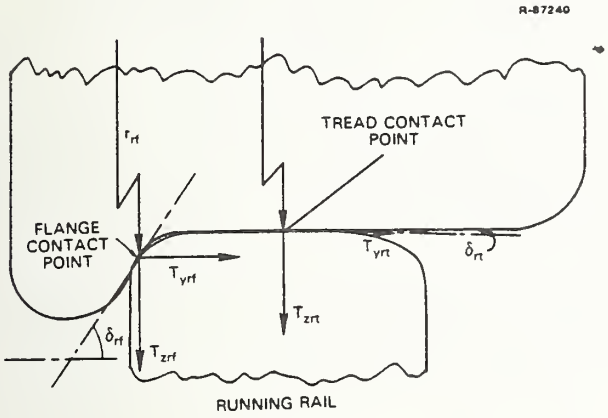

Figure 4.1-1 End View of Wheel and Rail with Second Contact Point on Flange Front

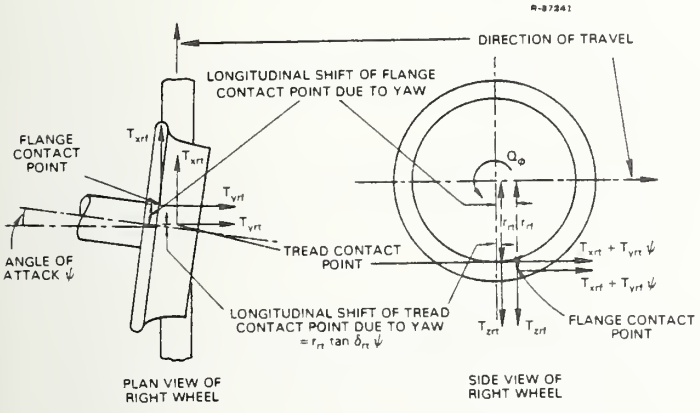

Figure 4.1-2 Forces and Torques Acting About Wheelset Axis with Second Point of Contact on Flange Front (Only Forces on Right Wheel are Shown)

In the other case, the second point of contact is on the back face of the flange. This situation occurs when a restraining rail is used on a curve (Figs. 4.1-3 and 4.1-4). The purpose of the restraining rail being to prevent or mitigate the flange contact which would otherwise occur on the lead axle wheel in contact with the high rail. The restraining rail achieves this by contacting the flange back of the lead axle wheel, which is in tread contact with the low rail and preventing further lateral displacement of the

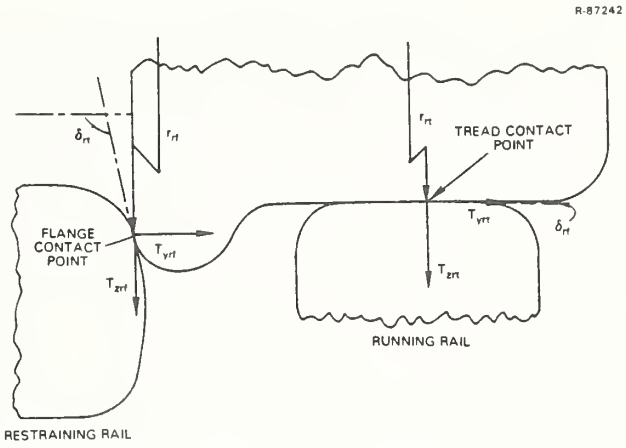

Figure 4.1-3 End View of Wheel and Rail with Second Contact Point on Flange Back

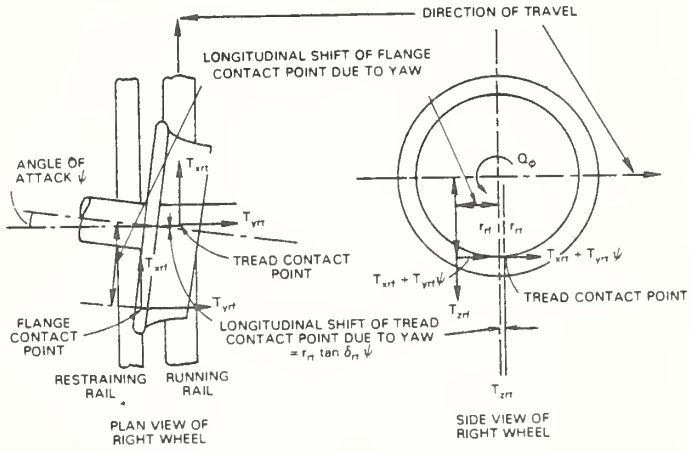

Figure 4.1-4 Forces and Torques Acting About Wheelset Bearing Axis with Second Contact Point on Flange Back (Only Forces on Right Wheel are Shown)

wheelset towards the high rail. This, then, represents a situation of two-point contact on the low rail wheel.

The example that is used now, in order to generate expressions for the creepages and hence, creep forces acting on an axle, is an axle which is in flange and, therefore, two-point contact on the right wheel and single-point contact with the tread on the left wheel.

4.2 CREEPAGE EXPRESSIONS

The situation of steady-state negotiation of a constant radius curve is considered. This means that there are no terms in the creepage expressions resulting from lateral or yaw velocity of the wheelset. The creepage expressions are:

$$\alpha_{1\ell} = \frac{\dot{\phi} r_{\ell}}{V} + 1 - \frac{\ell_o}{R_o} \qquad (4.2\text{-}1)$$

$$\alpha_{1rt} = \frac{\dot{\phi} r_{rt}}{V} + 1 + \frac{\ell_o}{R_o} \qquad (4.2\text{-}2)$$

$$\alpha_{1rf} = \frac{\dot{\phi} r_{rf}}{V} + 1 + \frac{\ell_o}{R_o} \qquad (4.2\text{-}3)$$

$$\alpha_{2\ell} = \frac{\dot{\phi} r_{\ell}}{V} \sec \delta_{\ell} \cdot \psi \qquad (4.2\text{-}4)$$

$$\alpha_{2rt} = \frac{\dot{\phi} r_{rt}}{V} \sec \delta_{rt} \cdot \psi \qquad (4.2\text{-}5)$$

$$\alpha_{2rf} = \frac{\dot{\phi} r_{rf}}{V} \sec \delta_{rf} \cdot \psi \qquad (4.2\text{-}6)$$

$$\omega_{3\ell} = - \frac{\dot{\phi} \sin\delta_{\ell}}{V} \qquad (4.2\text{-}7)$$

$$\omega_{3rt} = \frac{\dot{\phi} \sin\delta_{rt}}{V} \qquad (4.2\text{-}8)$$

$$\omega_{3rf} = \frac{\dot{\phi} \sin\delta_{rf}}{V} \qquad (4.2\text{-}9)$$

4.3 CREEP FORCES

The creep forces, occurring at the interface between wheel and rail at each point of contact are functions of the creepages, the ellipticity of the contact patch, T_3, the normal force on the contact patch and μ the coefficient of friction.

Kalker has developed a prediction method, known as "Duvorol", which predicts the relationship between creepages and creep forces to the point of saturation (Ref. 20). This method is able to predict accurately for cases that have a very high ellipticity, which is typical of the contact patches occurring on flange contact points. Using this method, a table of data has been generated which contains values of non-dimensional creep forces τ_1 and τ_2 for a range of non-dimensional creepage, spin and contact patch ellipticity. The creep forces are related to the non-dimensional creep forces by the following expressions:

$$T_1 = \mu T_3 \tau_1 \qquad (4.3\text{-}1)$$

$$T_2 = \mu T_3 \tau_2 \qquad (4.3\text{-}2)$$

This table of data is stored in the computer along with the wheel/ rail profile geometry data.

Knowledge of the wheelset lateral position, y, angle-of-attack ψ, and rotational speed $\dot{\phi}$ are sufficient for the creepage expressions (Eqs. 4.2-1 - 4.2-9) to be determined. The wheel/ rail profile geometry table then provides the contact patch geometry that is required to non-dimensionalize the creepages. A rapid search and interpolation routine is then used to calculate values of non-dimensional creep force at each point of contact. Before the creep forces T_1 and T_2 can be determined from Eqs. 4.3-1 and 4.3-2, it is necessary to know the normal force T_3 on each point of contact

$$T_{3\ell} = T_{z\ell}/(\cos\delta_{\ell} + \mu\tau_{2\ell} \sin\delta_{\ell}) \qquad (4.3\text{-}3)$$

$$T_{3rt} = T_{zrt}/(\cos\delta_{rf} - \mu\tau_{2rt} \sin\delta_{rt}) \qquad (4.3\text{-}4)$$

$$T_{3rf} = T_{zrf}/(\cos\delta_{rf} - \mu\tau_{2rf} \sin\delta_{rf}) \qquad (4.3\text{-}5)$$

For the left-hand wheel, where for this example there is only a single point of contact, a knowledge of the vertical wheel load $T_{z\ell}$ is sufficient to permit a determination of the normal force $T_{3\ell}$, and, hence, using Eqs. 4.3-1 and 4.3-2, the creep forces $T_{1\ell}$ and $T_{2\ell}$. However, for the right hand wheel, where there are two points of contact, it is necessary to know both the vertical loads T_{zrt} and T_{zrf}, supported by the tread and flange contact points, respectively, in order to determine the creep forces T_{1rt}, T_{1rf}, T_{2rt}, and T_{2rf}, which occur at the two points of contact. The full implication of this requirement will be discussed later.

Having obtained the creep forces in contact plane axes, they are now converted into an axis system which is fixed with respect to the track (Fig. 4.3-1). The sign convention for position displacements and forces with respect to this axis system is also shown in Fig. 4.3-1.

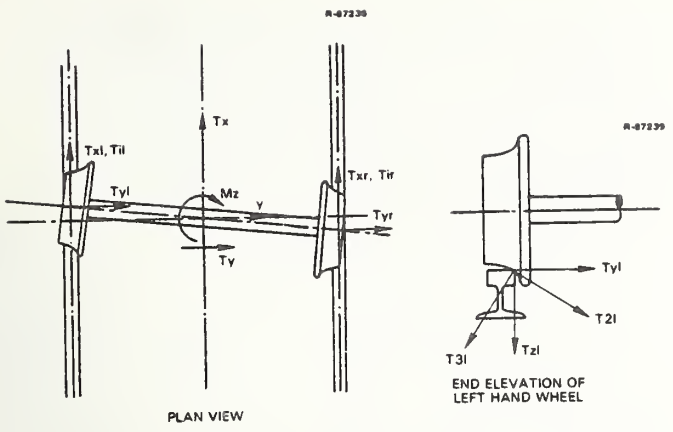

Figure 4.3-1 Axis System for Wheel/Rail Forces and Displacements

$$T_{xr} = T_{1rt} + T_{1rf} \qquad (4.3\text{-}6)$$

$$T_{x\ell} = T_{1\ell} \qquad (4.3\text{-}7)$$

$$T_{yr} = T_{2rt} \sec\delta_{rt} + T_{2rf} \sec\delta_{rf} + T_{zrt} \tan\delta_{rt} + T_{zrf} \tan\delta_{rf} \qquad (4.3\text{-}8)$$

$$T_{y\ell} = T_{2\ell} \sec\delta_{\ell} - T_{z\ell} \tan\delta_{\ell} \qquad (4.3\text{-}9)$$

In order to calculate M_Z, the yaw moment on the axle, it is necessary to take into account the contributions coming from the lateral forces. This occurs because the various contact points are offset longitudinally from a line radial to the curve (Figs. 4.1-2 and 4.1-4). This effect is most pronounced in the case of flange back contact with a restraining rail.

$$M_Z = \left[T_{x\ell} + T_{y\ell}\,\psi\left(1 - \frac{r_\ell}{\ell_o}\tan\delta_\ell\right) - T_{xrt} - T_{yrt}\,\psi\left(1 - \frac{r_{rt}}{\ell_o}\tan\delta_{rt}\right) - T_{xrf} - T_{yrf}\,\psi\left(1 - \frac{r_{rf}}{\ell_o}\tan\delta_{rf}\right)\right]\ell_o$$

4.4 WHEELSET ROTATIONAL SPEED

In Section 4.3, the requirement to know the magnitude of wheelset rotational speed $\dot{\phi}$, in order to determine the creepages and, hence, creep forces, was discussed. Since $\dot{\phi}$ itself is dependent upon the creep forces, an iterative procedure is used for its determination. In order to calculate $\dot{\phi}$, the torque balance of the wheelset must be considered (Figs. 4.1-2 and 4.1-4). The torque due to creep forces $Q_{\phi t}$ is given by

$$Q_{\phi t} = (T_{xrt} + T_{yrt}\,\psi - T_{zrt}\tan\delta_{rt}\,\psi)\,r_{rt} + (T_{xrf} + T_{yrf}\,\psi - T_{zrf}\tan\delta_{rf}\,\psi)\,r_{rf} + (T_{x\ell} + T_{y\ell}\,\psi + T_{z\ell}\tan\delta_{r\ell}\,\psi)\,r_\ell \qquad (4.4\text{-}1)$$

The contribution to the torque coming from the vertical wheel/rail forces T_{zrt}, T_{zrf}, and $T_{z\ell}$, are due to longitudinal movement of the points of contact, from vertically below the wheelset axis of rotation, when the wheelset is yawed as shown in Figs 4.1-2 and 4.1-4.

Using Eqs. 4.3-6 to 4.3-9, Eq. 4.4-1 is reduced to

$$Q_{\phi t} = (T_{1rt} + T_{2rt}\,\psi\sec\delta_{rt})\,r_{rt} + (T_{1rf} + T_{2rf}\,\psi\sec\delta_{rf})\,r_{rf} + (T_{1\ell} + T_{2\ell}\,\psi\sec\delta_{\ell})\,r_\ell \qquad (4.4\text{-}2)$$

If the wheelset is under the influence of braking or traction torques, then $Q_{\phi t}$, the torque due to creep forces is equal to the external torque applied from the braking or traction system. In the case of an unbraked and unpowered axle, $Q_{\phi t}$ is zero, except for a small torque due to bearing drag, but this is relatively small and, usually, can be neglected.

The obtaining of torque balance is an iterative procedure in which small adjustments in $\dot{\phi}$ are made. (The method used for this is described in detail in Ref. 18.)

4.5 PREDICTING WHEEL/RAIL FORCES IN TWO-POINT CONTACT

The predicted lateral force and yaw moment as a function of lateral displacement, for a wheelset with AAR cylindrical profiles in AREA115RE rail, are shown in Figs. 4.5-1 and 4.5-2.

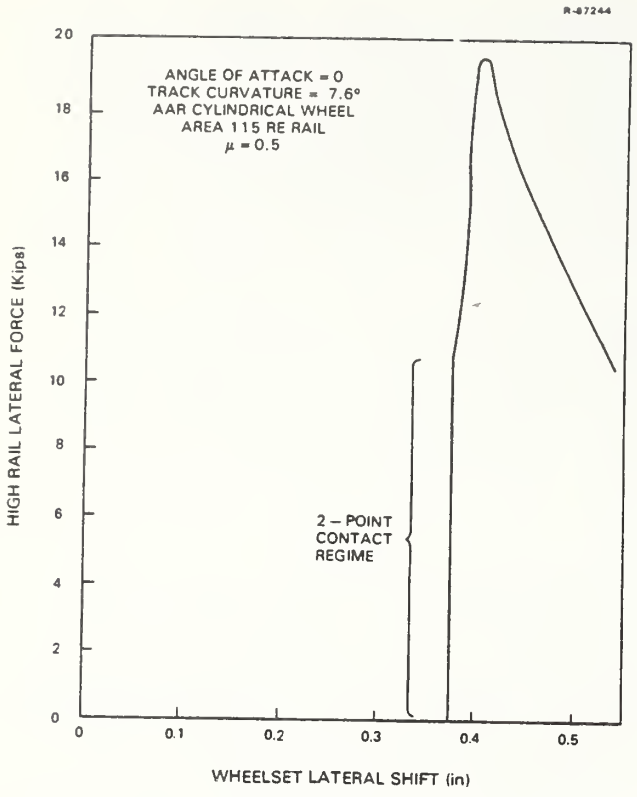

Figure 4.5-1 High Rail Lateral Force - Wheelset Lateral Shift

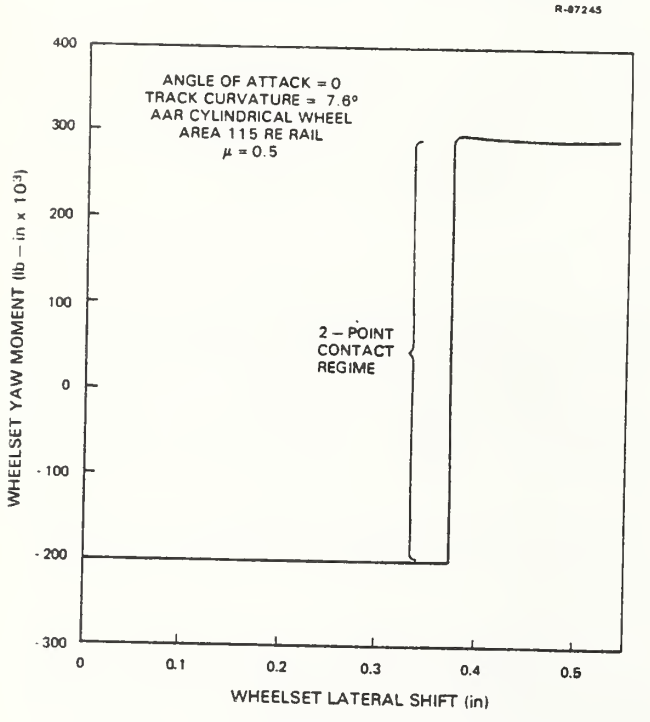

Figure 4.5-2 Wheelset Yaw Moment - Wheelset Lateral Shift

This wheel/rail profile combination is the one used at WMATA. This particular case is for a 7.6° curve with zero angles-of-attack. Flange contact first occurs at a lateral displacement of 0.375 in., which is when two-point contact occurs.

The regime of two-point contact is indicated on the figures and, in this regime both lateral force and yaw moment experience a change in magnitude without further lateral displacement. This regime starts from the condition where all the vertical load is supported by the tread contact point

$$T_{zrt} = T_{zr} \qquad (4.5\text{-}1)$$

$$T_{zrf} = 0 \qquad (4.5\text{-}2)$$

and ends at the condition where the vertical load on the tread has been reduced to zero and all the load is supported by the flange

$$T_{zrt} = 0 \qquad (4.5\text{-}3)$$

$$T_{zrf} = T_{zr} \qquad (4.5\text{-}4)$$

Although the lateral force and yaw moment cannot be separately defined for this lateral displacement, there is a unique relationship between them. In order to determine a point on this characteristic, a value is assumed for either the vertical or lateral force supported by the flange contact point. This permits a unique definition of the normal and tangential forces at both points of contact. In order to map the complete region of two-point contact, a range of either vertical or lateral flange forces needs to be used. This range starts from the condition where there is no load on the flange and therefore all the load is supported by the tread contact point, and ends at the condition where the load on the tread has just been reduced to zero and all the load is supported by the flange.

5. WHEEL/RAIL FORCE CHARACTERISTICS

Plots of axle yaw moment against lateral force provide a convenient means of comparing the characteristics of the various methods for predicting wheel/rail forces discussed in this paper. Figure 5-1 shows the results for the same case as that used for Figs. 4.5-1 and 4.5-2. This may be thought of as representing the situation approached by steering trucks with axles radial to the sharpest curve experienced during the track tests at WMATA. The difference in the characteristic for two-point, as compared with single-point contact, can be clearly seen. The essential feature of the difference is the significantly lower steering yaw moment for a given lateral force obtained with two point contact.

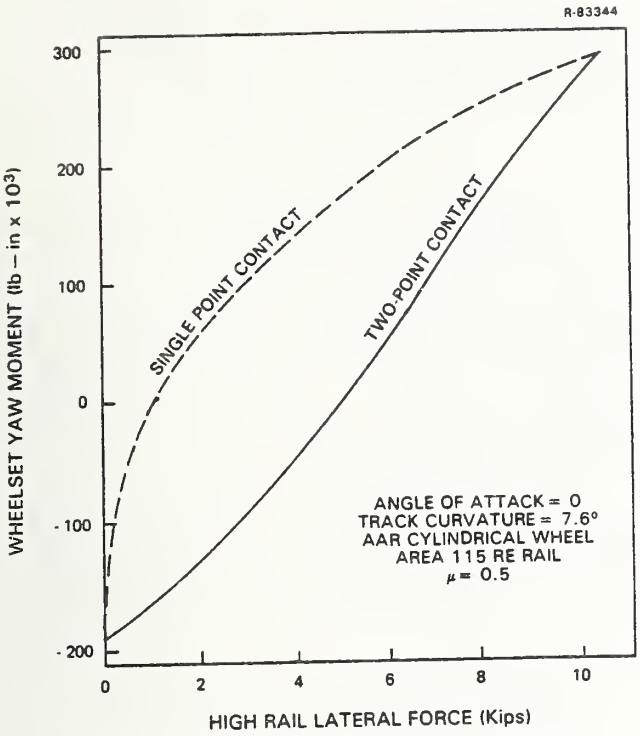

Figure 5-1 Wheelset Yaw Moment - High Rail Lateral Force

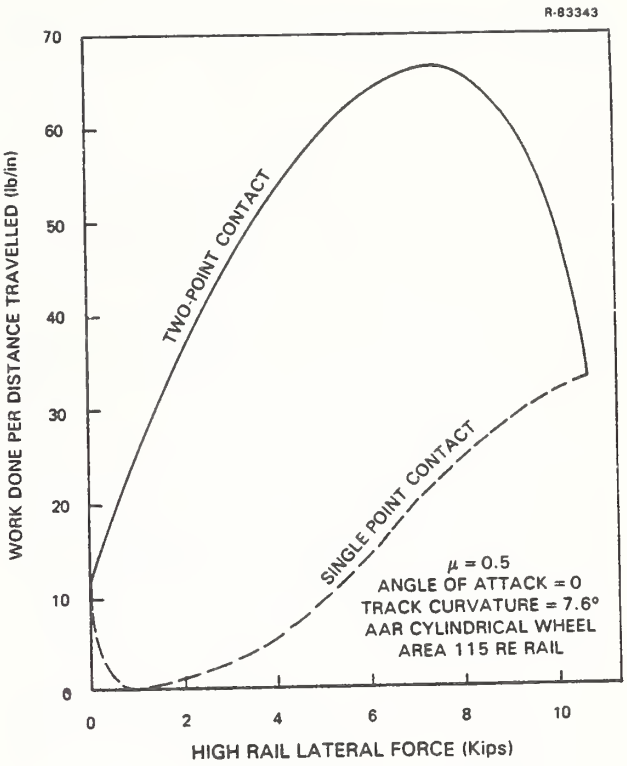

Figure 5-2 Work Done on Flanging Wheel - High Rail Lateral Force

When two points of contact are present on a single wheel, the rolling radius difference between the two points usually leads to longitudinal forces that are in opposition. This situation tends to reduce the net longitudinal force available from that wheel compared with a single-point contact situation. This in turn reduces the yaw moment which leads to the prediction of larger lead axle angles-of-attack in a steady-state curving calculation.

The work done in the contact patches during curve negotiation is receiving increasing acceptance as an indicator of curving performance. Work described in Ref. 18 shows that this parameter is related to wheel and rail wear and train resistance. Figure 5-2 shows the work done as a function of lateral force on the high rail for the same case as Fig. 5-1. The very large difference between the single and two-point contact characteristics is clearly demonstrated.

The plots of axle yaw moment against lateral force also provide a means of comparing the characteristics of different wheel/rail profile combinations.

Figure 5-3 shows yaw moment against lateral force characteristics for various wheel/rail profile combinations. This is for the case of a wheelset at zero angle-of-attack on a 7.6° curve where the rail cross section is a new AREA115RE rail. It can be seen that the AAR cylindrical wheel gives the the lowest yaw moment for a given lateral force throughout the entire range. The effect of increasing the wheel tread taper is to increase the yaw moment for a given lateral force. The reason for this increased yaw moment is associated with the reduction in radius difference between the two points of contact as the tread taper angle is increased.

Figure 5-4 is a repeat of the case illustrated in Fig. 5-3 except that the axle angle-of-attack is changed from zero to 0.55 degrees. This being approximately the angle-of-attack that would be obtained on the lead axle of a truck with a very stiff primary suspension on a 7.6° curve. For this case, the rate of increase in yaw moment with lateral force is less than for zero angle-of-attack. The AAR cyclindrical wheel is again producing the lowest yaw moment for a given lateral force.

For all of the profiles, a maximum lateral force of between 10.5 Kips and 11 Kips is obtained. A further increase in yaw moment is accompanied by a decrease in lateral force. The situation at which the lateral force is a maximum represents the point of impending derailment.

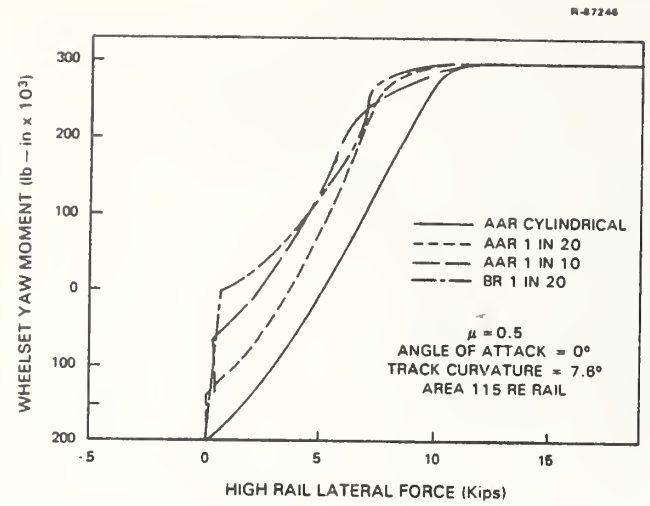

Figure 5-3 Wheelset Yaw Moment - High Rail Lateral Force for Various Wheel Profiles (0° Angle-of-Attack, New Rail)

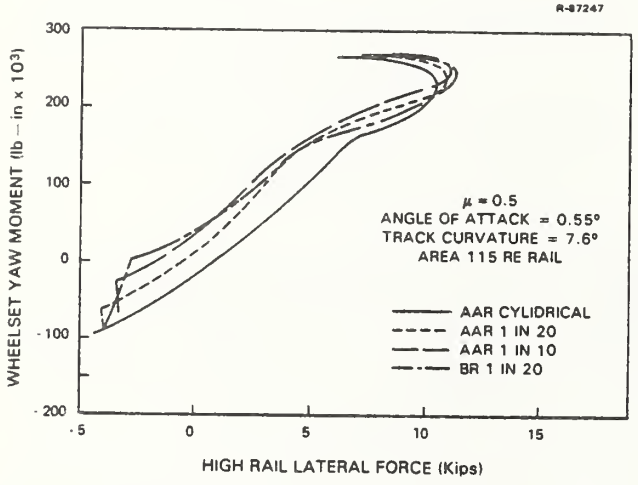

Figure 5-4 Wheelset Yaw Moment - High Rail Lateral Force for Various Wheel Profiles (0.55° Angle-of-Attack, (New Rail)

In Fig. 5-5, the effect is shown of changing from the new AREA115RE rail to a worn rail. The rail cross-section that is used was measured at a site on the high rail of curve 37 at WMATA. The gauge face wear at this site is typical of the average for the curve as a whole. Results are shown for an AAR cylindrical wheel at zero and 0.55 degree angle-of-attack. It can be seen that the effect of rail shape is quite significant. This is seen as a larger yaw moment with the worn rail, particularly in the case of zero angle-of-attack. This larger yaw moment is a result of the smaller radius difference between the two-points of contact with the worn rail.

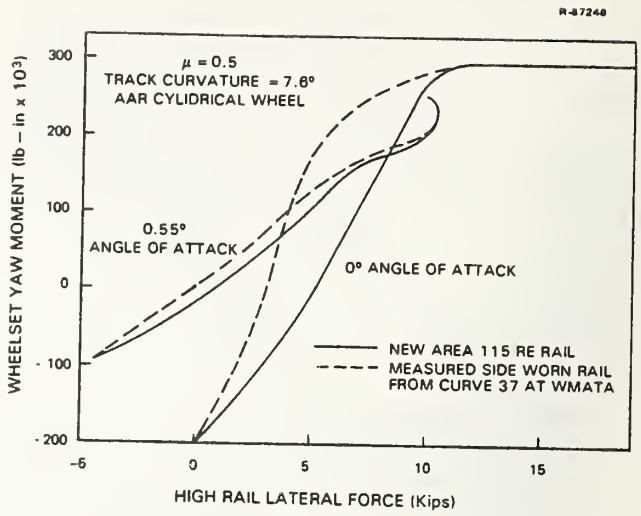

Figure 5-5 Wheelset Yaw Moment - High Rail Lateral Force for New and Worn Rail Profiles

6. STEADY-STATE CURVING ANALYSIS WITH TWO-POINT CONTACT

For a given wheelset lateral position, angle-of-attack and vertical load distribution, the method described in Section 4 will establish the forces that are generated between wheel and rail. When there is only a single point of contact between each wheel and rail, the steady-state curving problem consists of finding a set of wheelset lateral displacements and angles-of-attack which provide wheel/rail forces in equilibrium with the truck suspension forces, together with any externally applied forces.

Mainly as a result of the wheel/rail interaction, the equations describing the problem are highly nonlinear. The computational method that is used here assumes that, for any displacements, the equations are linear for small disturbances. Having made this assumption, the matrix equation that has to be solved is of the following simple form

$$[K]\ \{Y\} = \{F\} \qquad (6\text{-}1)$$

{Y} is a column matrix of wheelset lateral positions and angles-of-attack, for which a solution is sought. [K] is a square matrix, which contains terms associated with the stiffness constraints between the wheelsets and additional terms which come from the local linearizations of the wheel/rail interaction (Ref. 1). {F} is a column matrix of externally applied forces and additional terms, which are zero offsets associated with the linearization of the wheel/rail interaction (Ref. 1).

Solution of Eq. 6-1 is an iterative process where the terms associated with the local linearizations of the wheel/rail interaction are successively adjusted until balance is obtained.

In the case of two-point contact, the lateral displacement of the particular wheelset is no longer unknown. However, in order for the creep forces to be determined on the wheel in two-point contact, the vertical load on the flange as well as the tread must be known. The additional lateral force and yaw moment on the wheelset resulting from the second point of contact may be included in Eq. 6-1. These additional terms are T_{yrf}, the lateral force on the flange contact point and M_{zrf} the increment in yaw moment due to the forces occurring on the flange contact point. For ease of analysis, it is assumed that

$$M_{zrf} = C \cdot T_{yrf} \qquad (6\text{-}2)$$

If Eq. 6-1 is now rewritten, to include these additional terms and partitioned, we obtain

$$\begin{bmatrix} K_{11} & K_{12} & K_{13} \\ K_{21} & K_{22} & K_{23} \\ K_{31} & K_{32} & K_{33} \end{bmatrix} \begin{Bmatrix} y_1 \\ \psi_1 \\ y_3 \end{Bmatrix} = \begin{Bmatrix} F_1 \\ F_2 \\ F_3 \end{Bmatrix} + \begin{Bmatrix} 1 \\ C \\ 0 \end{Bmatrix} T_{yrf} \qquad (6\text{-}3)$$

where

y_1 is the known lateral displacement of the wheelset in two-point contact

ψ_1 is the angle-of-attack of the wheelset in two-point contact

y_3 are the lateral displacements and angles-of-attack of the wheelsets not in two-point contact.

Equation 6-3 can be rearranged to give

$$\begin{bmatrix} 1 & K_{12} & K_{13} \\ C & K_{22} & K_{23} \\ 0 & K_{32} & K_{33} \end{bmatrix} \begin{Bmatrix} T_{yrf} \\ \psi_1 \\ y_2 \end{Bmatrix} = \begin{Bmatrix} F_1 \\ F_2 \\ F_3 \end{Bmatrix} - \begin{Bmatrix} K_{11} \\ K_{12} \\ 0 \end{Bmatrix} y_1 \qquad (6\text{-}4)$$

This equation may be solved to yield values for all the displacements and the lateral force on the flange T_{yrf} for the known wheelset lateral displacement y_1.

There is a simple relationship between the lateral force on the flange T_{yrf} and the vertical force on the flange Tzrf.

$$T_{zrf} = T_{yrf} \frac{(1 - \mu\tau_{2rf} \tan\delta_{rf})}{(\mu\tau_{2rf} + \tan\delta_{rf})} \qquad (6\text{-}5)$$

Hence, the vertical load on the flange contact point T_{zrf} may be determined. This then permits a complete solution of the curving problem with two-point contact. This applies whether the second point of contact is on the front or back face of the flange.

The computer program that performs the steady-state curving predictions is arranged so that it does a preliminary calculation, which assumes only a single point of contact on each wheel. If the predicted wheelset lateral displacements for lead and trail axle are displacements which give only a single point of contact, then the correct solution has been obtained. However, if either of the wheelset lateral displacements is a value for which two-point contact is known to exist, then the single point contact predictions are used as the starting point for the full two-point contact solution which has been described in this section.

7. STEADY-STATE CURVING PREDICTIONS WITH SECOND POINT OF CONTACT ON FLANGE FRONT AND COMPARISON WITH EXPERIMENTAL RESULTS

The method of curving predictions, which is described in the previous section of this report, was used to make predictions of the curving behavior of the WMATA vehicle. Vehicle parameters used in this study are extracted from Table 7-1, which was presented previously in Ref. 1.

For all of these predictions, the coefficient of friction between wheel and rail at each of the contact points has been assumed to be equal to 0.5. The friction coefficient was not measured directly during the test program. It is in fact very difficult to obtain meaningful measurements of friction coefficient between wheel and rail, particularly at the contact point on the gauge face of the high rail. The value of 0.5 was deduced from the experimental measurements and computer predictions as being the most appropriate value. In particular, the lateral over a vertical force ratio on the lead axle low rail wheel, where there is

TABLE 7-1

UNLADEN WMATA CAR AND ROCKWELL TRUCK PARAMETERS

T-5152

		VALUES
	MASS PARAMETERS	
	Body Mass	130.5 lb-sec^2/in.
(2)	Car Body Yaw Inertia	$10.75 \cdot 10^6$ lb-in.-sec^2
(2)	Car Body Roll Inertia	$0.53 \cdot 10^6$ lb-in.-sec^2
	Truck Frame Mass	14.25 lb-sec^2/in.
	Truck Frame Yaw Inertia	10,500 lb-in.-sec^2
	Truck Frame Roll Inertia	4,600 lb-in.-sec^2
	Axle Mass	8.16 lb-sec^2/in.
	Axle Yaw Inertia	4,700 lb-in.-sec^2
	DAMPING PARAMETERS	
	Secondary Vertical Damping (per truck)	272 lb-sec/in.
	Secondary Lateral Damping (per truck)	236 lb-sec/in.
	Secondary Roll Damping (per truck)	$0.245 \cdot 10^6$ lb-in.-sec/rad
(1)*	Secondary Yaw Pivot Friction (per truck)	90,000 lb-in.
	STIFFNESS PARAMETERS	
(2)	Secondary Vertical Stiffness (per truck)	3405 lb/in.
(2)	Secondary Lateral Stiffness (per truck)	3250 lb/in.
*	Secondary Yaw Stiffness (per truck)	$31.2 \cdot 10^6$ lb-in./rad
(2)	Secondary Roll Stiffness (per truck)	$2.17 \cdot 10^6$ lb-in./rad
	STANDARD PRIMARY BUSHING	
(1)	Primary Vertical Stiffness (per wheel)	74,000 lb/in.
(1)	Primary Lateral Stiffness (per wheel)	62,300 lb/in.
(1)	Primary Longitudinal Stiffness (per wheel)	115,000 lb/in.
	MODIFIED PRIMARY BUSHING	
(1)	Primary Vertical Stiffness (per wheel)	116,000 lb/in.
(1)	Primary Lateral Stiffness (per wheel)	32,000 lb/in.
(1)	Primary Longitudinal Stiffness (per wheel)	29,000 lb/in.
	GEOMETRICAL PARAMETERS	
	Longitudinal Semi-Spacing of Truck Centers	312 in.
	Lateral Semi-Spacing of Air Springs	25.25 in.
	Vertical Height of Car C.G. Above Rail	55.5 in.
	Vertical Height of Secondary Suspension Roll Center Above Rail	11.5 in.
	Vertical Height of Truck C.G. Above Rail	11.5 in.
	GEOMETRICAL PARAMETERS	
	Semi-Wheelbase of Truck	43.5 in.
	Lateral Semi-Spacing of Primary Bushes	22.63 in.
	Lateral Semi-Spacing of Wheel/Rail Contact Patches	30 in.
	Wheel Radius	14 in.
	OTHER PARAMETERS	
	Axle Load	18,500 lbs
	Lateral Creep Coefficient	$1.33 \cdot 10^6$ lbs
	Longitudinal Creep Coefficient	$1.46 \cdot 10^6$ lbs

*Linearized values of secondary yaw damping and stiffness were obtained from the secondary yaw pivot friction torque and secondary yaw stiffness using a sinusoidal describing function method.

(1)From shop test measurements.

(2)Computed from measured carbody on secondary suspension modal frequencies.

only a single point of contact, was used. The value of 0.5 for the coefficient of friction may appear high. However, the majority of the tighter curves used in the test program were in tunnels and, therefore, the rails were always dry.

Initially the predictions were carried out for the three wheel profiles that were used in the test program (AAR cylindrical, BR 1 in 20 and AAR 1 in 10) running on new AREA115RE rail.

On sharp curves most trucks adopt an attitude where the lead axle has a relatively large angle-of-attack, with the wheel on the high rail side being in flange contact with the gauge face of the rail. The trailing axle usually has a relatively small angle-of-attack and is not in flange contact. If the curve is sharp enough then the trailing axle will run in flange contact with the low rail. However, for the range of curvatures that are being considered here the trailing axle will not be in flange contact. Because of the large angle-of-attack and flange contact on the lead axle, the lead axle wheel/rail forces are of most interest. Therefore, the results of the study are presented in terms of lead axle high rail lateral force and lead axle yaw moment as a function of track curvature. The vehicle is assumed to be traveling at the balance speed for the curve.

Figure 7-1 presents the results for the WMATA vehicle with the standard stiff primary suspension bush. It can be seen that the AAR cylindrical profile gives higher lateral force and lower yaw moment than the other wheel profiles, particularly in the range of track curvature up to 7°-8°. The AAR 1 in 10 and BR 1 in 20 profiles give very similar results throughout the range of track curvature. With all three wheel profiles, the lead axle yaw moment reaches a maximum at approximately 8° of track curvature.

The use of a primary suspension with a reduced longitudinal stiffness gives a lower yaw stiffness between the axle and truck frame, which permits a reduction of the lead axle angle-of-attack in a sharp curve. This is achieved by allowing the axle to yaw relative to the truck frame through the action of the yaw moment developed through the wheel/rail interaction forces.

The case of a vehicle with the soft primary bush running on design case rails is considered in Fig. 7-2. The primary stiffnesses in this case

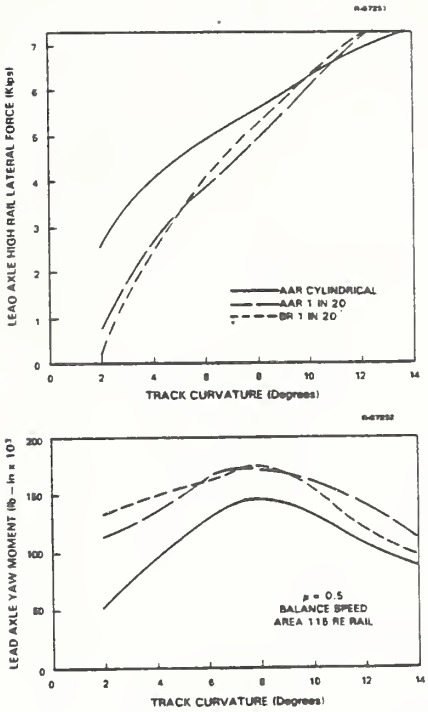

Figure 7-1 Predicted Lead Axle High Rail Lateral Force and Yaw Moment - Track Curvature (Stiff Primary Suspension, New Rail), Effect of Wheel Profile

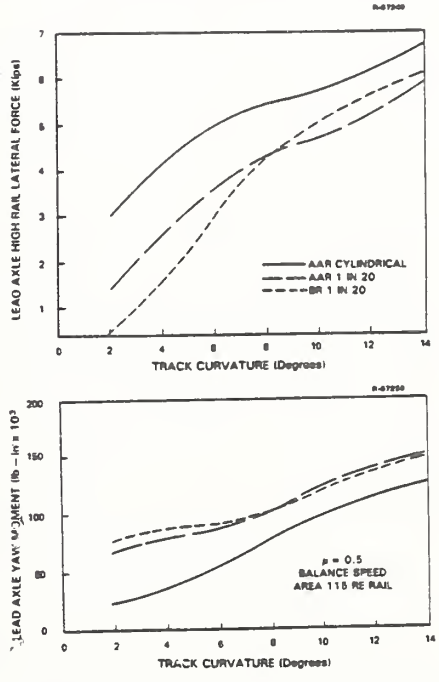

Figure 7-2 Predicted Lead Axle High Rail Lateral Force and Yaw Moment - Track Curvature (Soft Primary Suspension, New Rail), Effect of Wheel Profile

are presented in Table 7-1. Again the AAR cylindrical profile gives higher lateral forces and lower yaw moments than the other two wheel profiles. This situation now extends right up to the maximum curvature that was considered, 14°. The AAR 1 in 10 and BR 1 in 20 gives similar yaw moments throughout the range of track curvature. However, the BR 1 in 20 gives lower predicted lateral force below about 8° of curvature and the AAR 1 in 10 gives lower lateral forces above 8°.

The predictions are now repeated for the AAR cylindrical profile and the BR 1 in 20 profile except that the rail profile is a measured profile which is typical of the average profile on curve 37 at WMATA. This is a 7.6° curve with a significant amount of gauge face wear on the high rail.

Figure 7-3 presents predicted results for the vehicle with the standard stiff primary suspension. Also shown are the measured results for lead axle, high rail, lateral force at balance speed. The predictions are now in much better agreement with the measurements for the smaller curvatures up to about 5°. However, for the sharpest curve used in the test program, which was 7.6°, the predictions suggest less improvement in changing to the BR 1 in 20 profile than do the measurements. The yaw moment predictions indicate a maximum yaw moment at 7° track curvature for the AAR cylindrical profile and 6° for the BR 1 in 20 profile.

The results for the vehicle, with the modified soft bush, running on the measured rail profile, are shown in Fig. 7-4. There is good agreement between the measured and predicted results, which show a substantial reduction in lateral force in changing from the AAR cylindrical profile to the BR 1 in 20.

Figure 7-5 shows the effect of running at 5 in. below and 5 in. above balance speed. The case considered here is the vehicle with the modified primary suspension and AAR cylindrical wheel profiles running on the measured worn rails. Throughout the range of track curvature, the lateral force is increased by running above balance and decreased by running below balance. The lead axle yaw moment is hardly affected by changing speed.

In Figure 7-6 the same case is considered except that the wheel profile is changed to the BR 1 in 20 profile. Again the lateral force is increased by running above balance speed and decreased by running below balance speed. The yaw moment shows a small

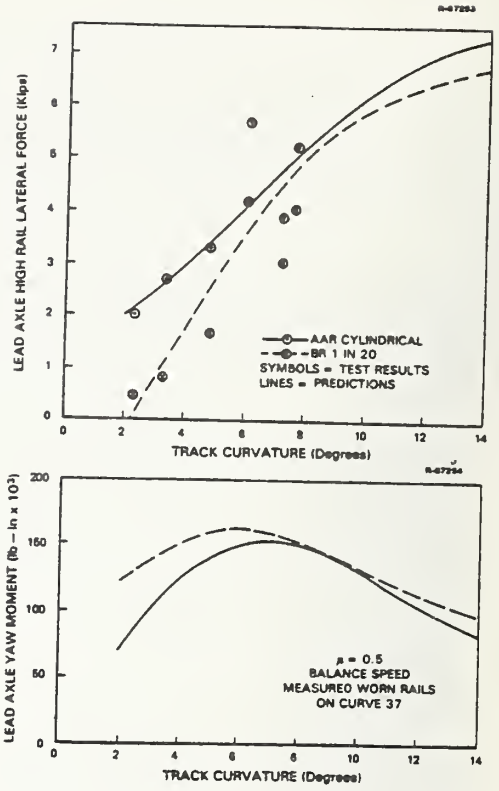

Figure 7-3 Lead Axle High Rail Lateral Force and Yaw Moment - Track Curvature (Stiff Suspension, Measured Worn Rails), Effect of Wheel Profile

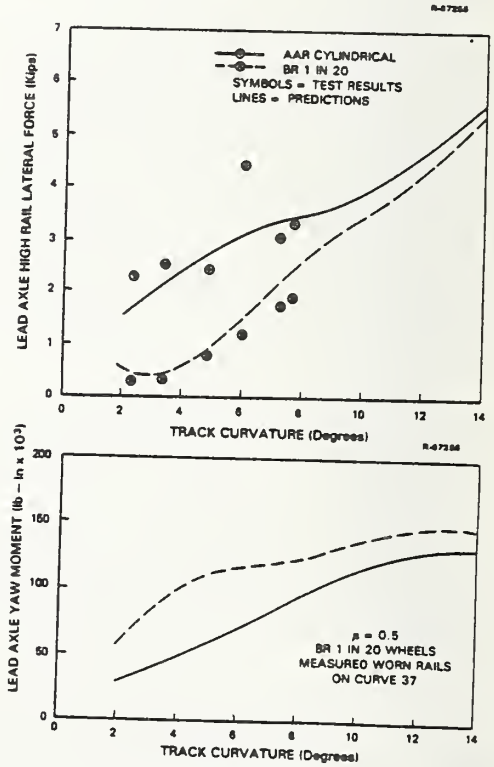

Figure 7-4 Lead Axle High Rail Lateral Force and Yaw Moment - Track Curvature (Soft Suspension, Measured Worn Rails), Effect of Wheel Profile

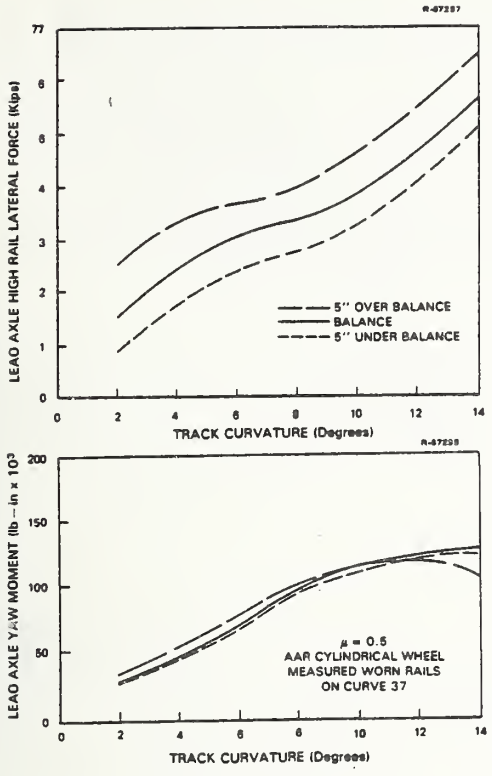

Figure 7-5 Predicted Lead Axle High Rail Lateral Force and Yaw Moment - Track Curvature (Soft Suspension, Measured Worn Rails, AAR Cylindrical Wheel), Effect of Speed

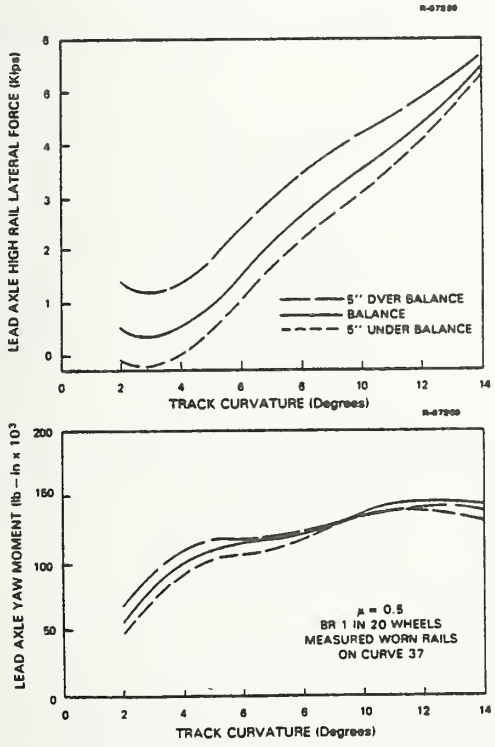

Figure 7-6 Predicted Lead Axle High Rail Lateral Force and Yaw Moment - Track Curvature (Soft Suspension, Measured Worn Rails, BR 1 in 20 Wheel), Effect of Speed

increase with increasing speed for curvatures below about 8°.

8. STEADY-STATE CURVING PREDICTIONS WHERE SECOND POINT OF CONTACT IS BETWEEN A RESTRAINING RAIL AND THE FLANGE BACK

On the very sharp curves where restraining rails are used, the lead axle will have a very large angle-of-attack. The direction of this angle is such that the lateral wheel/rail forces cause the axle to move towards contact with the high rail.

When a restraining rail is used, contact occurs between the back face of the flange of the lead axle wheel on the low rail side of the curve and the guard face of the restraining rail. This situation normally prevents flange contact with the gauge face of the high rail.

When the track curvature is large enough, flange contact will occur between the trailing axle wheel running against the low rail. For the WMATA truck this occurs at about 15° track curvature. The analytic modeling of this two-point contact situation has been described in Section 4 of this report. In this section the results of a theoretical steady state curving study are presented.

The vehicle that is considered here is the standard WMATA vehicle with the stiff primary suspension. The vehicle parameters are contained in Table 7.1.

The rail configuration that has been used in the study is the arrangement used on the Tight Turn Loop at the Transportation Test Center in Pueblo, Colorado. The running rails are design case AREA119RE rail which are at 56.5 in. gauge and canted at 1 in 40 to the vertical. The restraining rail is ASCE85 lying on its side with a nominal 2 in. gap between the guard face and the gauge face of the low rail. The restraining rail is positioned so that its upper face is approximately 0.75 in. above the head of the running rail. With this geometry, the point of contact on the flange back is approximately 4.4 in. ahead of the axle axis of rotation and approximately 0.45 in. above the rail head.

Predictions have been carried out for a range of track curvatures from 5°-40° at balance speed and speeds that represent 4 in. above and below balance. The coefficient of friction at all points of contact has been assumed to be equal to 0.5.

Figure 8-1 shows the predicted lateral forces on the wheels at high and low rails as a function of track curvature. These lateral forces acting upon the wheelset are assumed positive to the right (in the direction towards the center of the curve). Vertical forces are assumed positive downwards. At the high rail, the magnitude of the lateral force increases to approximately 10° curvature and is then approximately constant throughout the range of track curvature up to 40°. At balance speed a magnitude of approximately 4 Kips is predicted, increasing to just below 5 Kips at 5 in. above balance, and decreasing to approximately 3 Kips at 5 in. below balance.

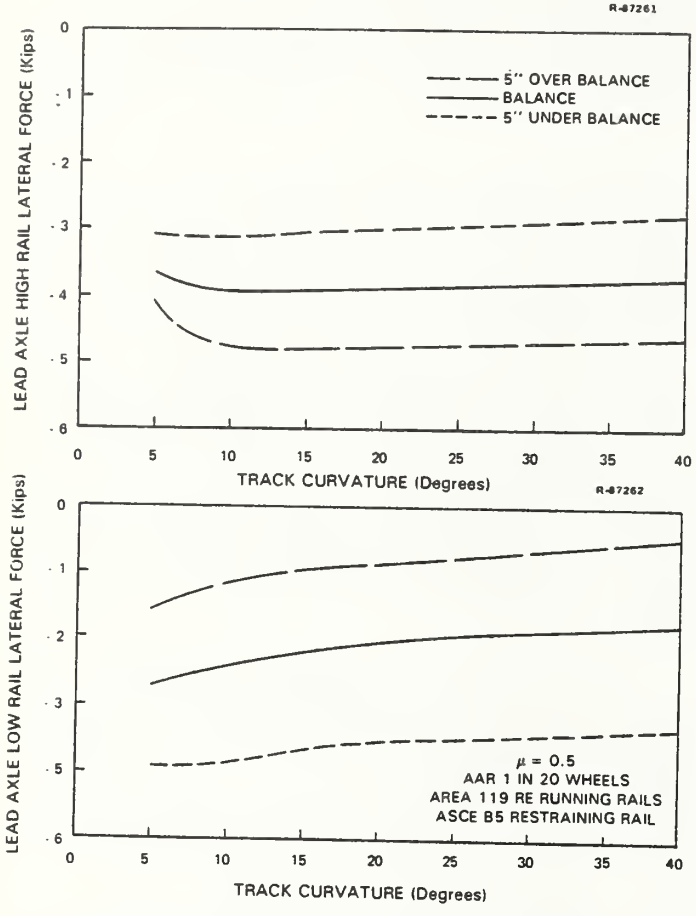

Figure 8-1 Predicted Lead Axle High and Low Rail Lateral Forces - Track Curvature (Stiff Suspension, Restraining Rail), Effect of Speed

At the low rail, the magnitude of the lateral force on the wheel tread reduces with increasing curvature, and with speed above balance. This reduction is due to the smaller vertical load on the wheel tread as more vertical load is transferred to the flange back with increasing curvature. In addition, running at above balance speed reduces the total vertical load supported by the low rail and restraining rail.

The predicted lateral and vertical forces on the flange back from the restraining rail are illustrated in Fig. 8-2. Above 10°, the predicted lateral force is almost constant with increasing curvature. A magnitude of approximately 10 Kips lateral force is predicted, which increases to about 10.5 Kips at 5 in. above balance and reduces to about 9 Kips at 5 in. balance below balance speed.

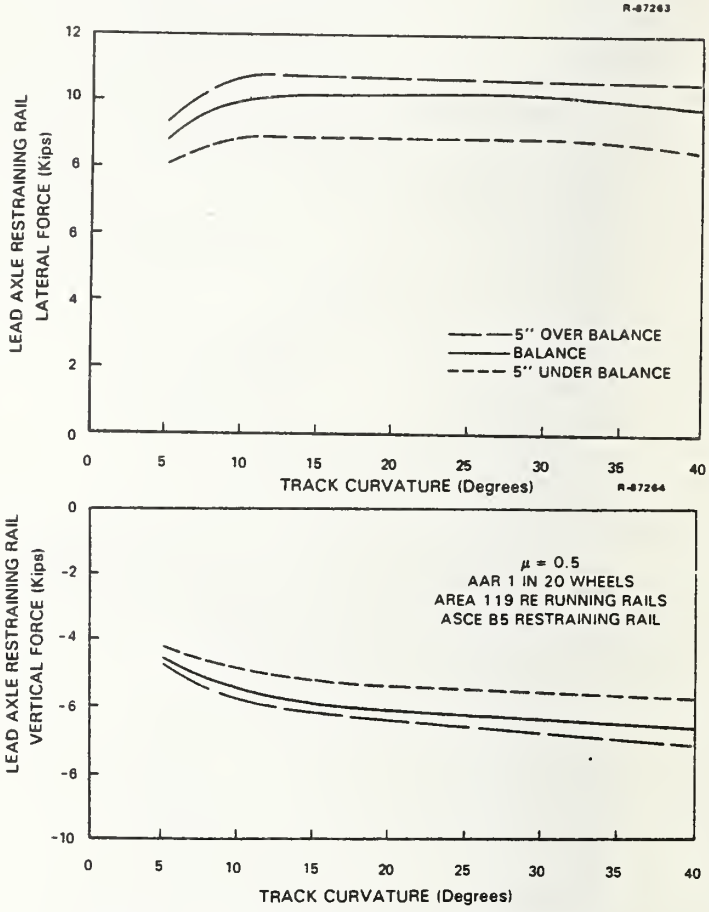

Figure 8-2 Predicted Lead Axle Restraining Rail Lateral and Vertical Forces - Track Curvature (Stiff Suspension, Restraining Rail), Effect of Speed

The vertical load supported by the restraining rail increases steadily in magnitude with increasing curvature. Increase in speed also causes an increase in vertical load supported. Typically, the vertical load on the restraining rail is approximately 6 Kips.

Figure 8-3 shows the predicted axle yaw moments for the lead and trail axles. The predicted yaw moment on the lead axle is small for all curvatures and speeds. There is a large negative yaw moment on the trailing axle tending to resist the curve rotation. At balance speed its magnitude increases to a maximum of 300×10^3 lb-in. at about

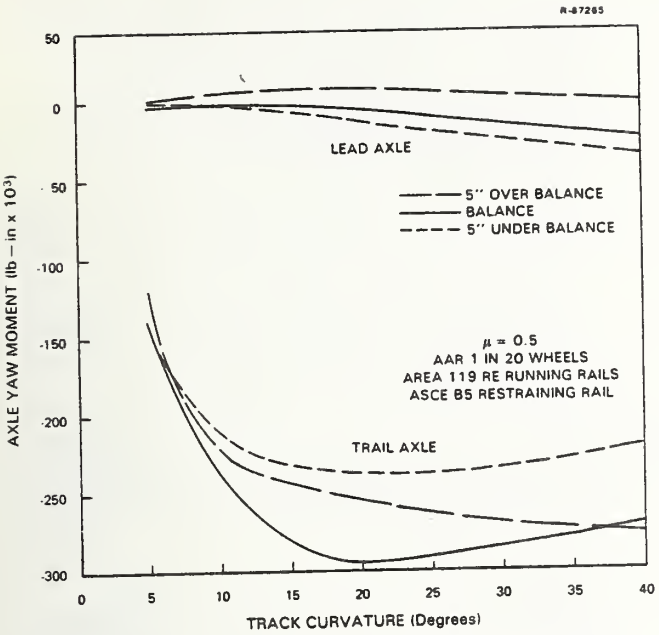

Figure 8-3 Predicted Lead and Rail Axle Yaw Moment - Track Curvature (Stiff Suspension, Restraining Rail), Effect of Speed

20° curvature. In general, increasing or decreasing the speed, relative to balance speed, causes a reduction in the magnitude of the trail axle yaw moment.

In Fig. 8-4, the complete system of forces on the truck is shown. This is for the case of 20° track curvature at balance speed. It can be seen that both of the axle yaw moments are in the same direction as the yaw torque coming from the truck yaw pivot. These three moments give a net moment of 365×10^3 lb-in. This moment is balanced by equal and opposite net lateral forces of 4.4 Kips on each axle. In this case there is a lateral force of 10.2 Kips on the flange back of the lead axle low rail wheel. The trail axle low rail wheel is also in two-point contact. In this case the second point of contact is on the flange front with a lateral force of 3.7 Kips.

9. CONCLUSIONS

Experimental results from a recent test program performed at WMATA have shown significant errors in the predictions of curving behavior from a method which assumes only a single point of contact between each wheel and rail. In particular, changes in curving forces due to different wheel profiles were poorly predicted.

The new wheel and rail profile combinations, in common use in the U.S.A.

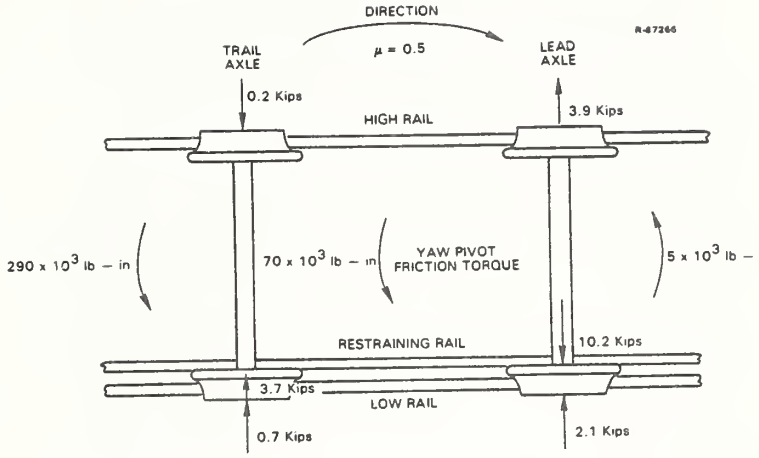

Figure 8-4 Complete System of Forces and Moments on Truck at Balance Speed (20° Curve with Restraining Rail)

and many other parts of the world, give two points of contact at the leading axle wheel in contact with the high rail on many curves. Also, when a restraining rail is used on a curve, two point contact occurs at the leading axle wheel on the low rail side of the curve. In this case, the second point of contact is on the flange back. These two-point contact situations have now been modeled and, in the cases where they can be compared with experimental results, show much better agreement.

The large reduction in high rail lateral force that was obtained with the BR 1 in 20 profile compared with the AAR cylindrical profile, during the curving tests at WMATA is now reasonably well predicted. This is particularly true in the case where a soft primary suspension was used. These results show the significant advantage of a wheel profile that gives a single point of contact under most conditions. This advantage is seen in terms of reduced wheel/rail forces and reduced work done in the contact between wheel and rail. This will lead to reduced wheel/rail wear and train resistance.

The capability now exists for predicting the curving behavior of vehicles in the presence of a restraining rail. An experiment is being conducted which should permit the validity of this prediction to be determined.

10. RECOMMENDATIONS

This work has indicated that significant reductions in wheel/rail wear and train resistance in curves would probably be available from wheel profiles which give only a single point of contact with the rail. The analytic model described in this report provides

the capability for studying the effects of wheel profile on wheel and rail wear and train resistance. Such a study could lead to the determination of more effective wheel profiles for American Railroads.

The capability now exists for predicting the effect of restraining rails on curving behavior. Use of the analytic model would allow the effects of variations in restraining rail geometry to be determined. This would be a very cost effective means of optimizing the geometry of the restraining rail and flange back for minimum wheel/rail wear and train resistance on sharp curves.

REFERENCES

1. Elkins, J.A., and Gostling, R.J., "A General Quasi-Static Curving Theory for Railway Vehicles," Proceedings from 5th VSD-2nd IUTAM Symposium, Vienna, September 1977.

2. Elkins, J.A., "Analytical Studies of Curving Forces and Hunting Stability and Related Support for WMATA Phase II Truck Test," Report No. UMTA, June 1982.

3. Porter, S.R.M., "The Mechanics of a Locomotive on Curved Track," The Railway Gazette, London, 1935.

4. Mackenzie, J., "Proceedings of Institute of Civil Engineers," Vol. LXXIV, pp. 1-57, 1883.

5. Wickens, A.H., "The Dynamics of Railway Vehicles on Straight Track: Fundamental Considerations of Lateral Stability," Proceedings Institute of Mechanical Engineering/Vol. 180, Part 3F, pp. 29-44 and p. 150, 1965.

6. Boocock, D., "The Steady-State Motion of Railway Vehicles on Curved Track," Journal of Mechanical Engineering Science, Vol. II, No. 6, 1969.

7. Newland, D., "Steering Characteristics of Bogies," The Railway Gazette, London, 1968.

8. Kalker, J.J., "On the Rolling Contact of Two Elastic Bodies in the Presence of Dry Friction," (plus table book Doctoral Thesis, Delft, 1967.

9. Gilchrist, A.O., and Brickle, B.V., "A Re-Examination of the Proneness to Derailment of a Railway Wheelset," Journal of Mechanical Engineering Science, Vol. 18, No. 3, pp. 131-141, 1976.

10. Sweet, L.M., and Sivak, J.A., "Nonlinear Wheelset Forces in Flange Contact - Part 1: Steady-State Analysis and Numerical Results," Journal of Dynamic Systems, Measurement and Control, Vol. 101, No. 3, September 1979.

11. Smith, K.R., MacMillan, R.D., and Martin, G.C., "Two, Three, and Four Axle Rigid Truck Curve Negotiation Model," International Government Industry Research Program of Track-Train Dynamics, administered by Association of American Railroads, 1975.

12. Doyle, G.R., "Conventional Versus Self-Steering Radial Trucks for High-Speed Passenger Trains," ASME Paper 79/RT/3, April 1974.

13. Sweet, L.M., Sivak, J.A., and Putman, W.F., "Nonlinear Wheelset Forces in Flange Contact - Part 2: Measurements Using Dynamically Scaled Models," Journal of Dynamic Systems, Measurement and Control, Vol. 101, No. 3, September 1979.

14. Apparao, T., "Digital Simulation of the Curve Entry Dynamics of a Rail Transit Vehicle," 4th Symposium on Engineering Applications of Solid Mechanics, Mississauga, Ontario, September 1978.

15. Phillips, C., Weinstock, H., Greif, R., and Thompson, III, W.I., "Measurements of Wheel/Rail Forces at the Washington Metropolitan Area Transit Authority, Vol. I, Analysis Report," Report No. UMTA-MA-06-0025-80-6, July 1980.

16. Ahlbeck, D.R., Harrison, H.D., and Tuten, J., "WMATA Wheel/Rail Force Measurement, Vol. II, Test Report," Report No. UMTA-MA-06-0025-80-7, February 1980.

17. Weinstock, H., and Greif, R., "Analysis of Wheel/Rail Force and Flange Force During Steady-State Curving of Rigid Trucks," Report No. UMTA-MA-06-0025-80-8, September 1980.

18. Elkins, J.A., and Allen, R.A., "Testing a Transit Vehicle for Wheel and Rail Wear," presented at ASME Winter Annual Meeting, Washington, D.C., Paper No. 81-WA/DSC-19, November 1981.

19. Elkins, J.A., and Eickhoff, B.M., "Advances in Nonlinear Wheel/Rail Force Prediction Methods and Their Validation," Journal of Dynamic Systems, Measurement and Control, Vol. 104, No. 2, June 1982.

REFERENCES (Continued)

20. Tjoeng, A.S.K.S., and Kalker, J.J., "User's Manual for the Program "Duvorol" in Algol 60 & Fortran for the Computation of Three-Dimensional Rolling Contact with Dry Friction," Delft TM, Report, Dept. of Mathematics, (1980).

APPENDIX

REPORT OF NEW TECHNOLOGY

No patentable item has been found in the work performed and described in this report. However, it contributes to the state-of-the-art in the area of rail vehicle curving simulation.

In particular, a new algorithm is presented which provides an accurate simulation of a rail vehicle truck in steady curving when the wheel and rail profiles lead to two points of contract on any wheel, including flange back contact with a restraining rail.

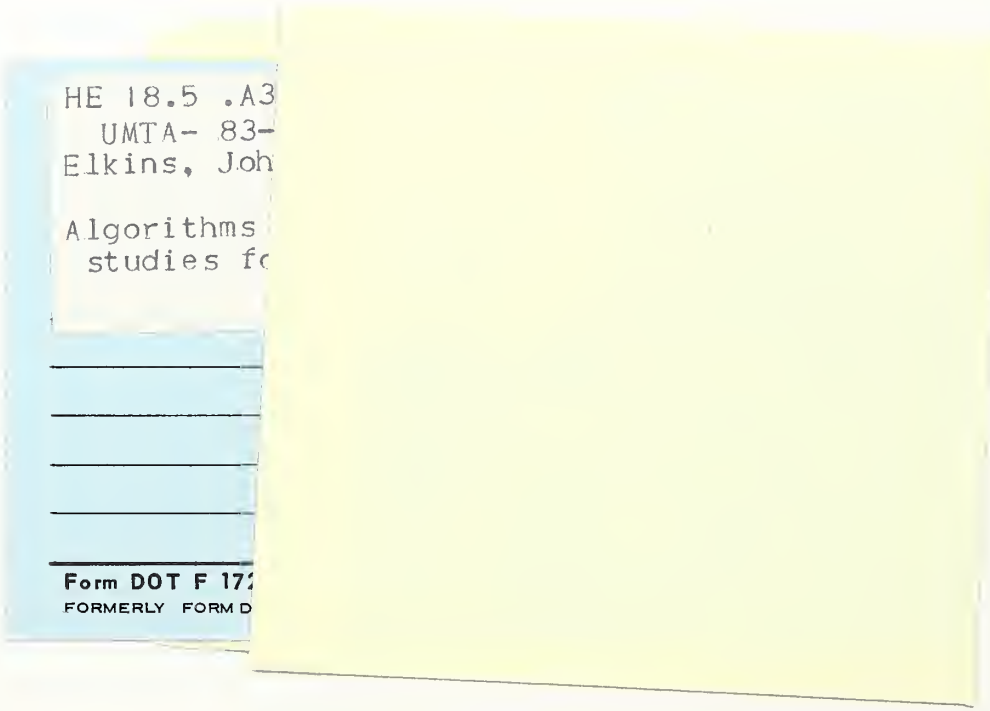

U.S. Department
of Transportation

**Research and
Special Programs
Administration**

Kendall Square
Cambridge, Massachusetts 02142

Postage and Fees Paid
Research and Special
Programs Administration
DOT 513

Official Business
Penalty for Private Use $300